Catalysis Today 147S (2009) S265–S270

Contents lists available at ScienceDirect

Catalysis Today

journal homepage: www.elsevier.com/locate/cattod

Analytical investigations on ageing phenomena of catalytic exhaust gas aftertreatment components

P. Lanzerath *, A. Guethenke, A. Massner, U. Gaertner

Daimler AG, Department TP/PMA, Mercedesstr.137, 70546 Stuttgart, Germany

ARTICLE INFO

Article history:
Available online 3 August 2009

Keywords:
Exhaust gas aftertreatment
Catalyst deactivation
Thermal ageing
Chemical poisoning

ABSTRACT

Upcoming emission limits for commercial vehicles cannot be maintained solely by modern combustion methods, optimized fuel injection systems and exhaust gas recirculation. In addition, combined exhaust gas aftertreatment systems are necessary. Over engine lifetime, performance deterioration of the exhaust gas aftertreatment systems can be observed. This is influenced by system design as well as operating strategies. The performance deterioration of catalysts is caused by thermal and chemical phenomena. Thermal ageing effects in a combined aftertreatment system containing a diesel particulate filter (DPF) are dominated by the filter active regeneration strategy. Chemical poisoning of the catalysts is caused primarily by engine oil.

Content of this study is the analysis of diesel oxidation catalysts from combined aftertreatment systems with varying operation time, but the same total PGM (Platinum Group Metal) loading. The catalysts are investigated regarding deterioration phenomena caused by thermal ageing and chemical poisoning. The catalytic conversion deterioration is correlated with the active DPF regeneration history of the components. As further methods BET, XRF, XRD and FESEM-EDX are applied. A correlation between specific catalyst surface as well as Pt particle size and active DPF regeneration history is investigated. Also, oil consumption and accumulation of poisoning elements on the catalyst surface are analyzed. The determination of clear correlations regarding thermal and chemical ageing phenomena is complicated by the large number of influence factors, as catalysts systems from on-road vehicles with different vehicle weight, operation time, total lube oil consumption and number of active DPF regenerations were analyzed.

1. Introduction

Stricter emission legislation in Europe and the USA leads to an increasing development of exhaust gas aftertreatment systems. The durability of catalytic performance over lifetime is essential for fulfilling the emission limits. However with increasing operation time, catalytic activity deteriorates. This is of particular importance in commercial vehicles because of long vehicle lifetimes and high mileages.

Generally a diesel oxidation catalyst (DOC) is used in an aftertreatment system to reduce gaseous HC- and CO-emissions. With the introduction of diesel particulate filters (DPF) and selective catalytic reduction (SCR) catalysts, DOCs obtain more responsibilities. To burn off the accumulated soot on a DPF, hydrocarbons can be injected into the exhaust stream and converted on a DOC upstream of the DPF to increase the exhaust gas temperature (approximately to 600 °C).

Additionally, the oxidation of NO to NO_2 on the DOC enhances the performance of downstream aftertreatment components. A higher NO_2 content in the exhaust gas facilitates the passive regeneration of soot on the DPF and also leads to an improved NO_x conversion on an SCR catalyst. With operation time, the oxidation rate of NO to NO_2 on the DOC decreases. This is mainly influenced by the number of active DPF regenerations and thereby high temperature exposure as well as by the accumulation of poisoning elements from lubrication oil.

2. Deactivation of diesel oxidation catalysts

The decrease in catalytic activity of a DOC is mainly caused by different chemical and physical effects, which result in structural and compositional changes of the catalyst surface. Thermal deactivation is caused by the sintering and agglomeration of noble metal components as well as the sintering of washcoat surface area. Chemical deactivation is effected by the accumulation of poisoning elements or other deposits on the catalyst [1,2].

Sintering and coalescence of active sites caused by high temperatures lead to an activity loss of the noble metal surface.

* Corresponding author. Tel.: +49 711 17 55619; fax: +49 711 3052 196855.
E-mail address: peter.lanzerath@daimler.com (P. Lanzerath).

0920-5861/$ – see front matter © 2009 Elsevier B.V. All rights reserved.
doi:10.1016/j.cattod.2009.07.028

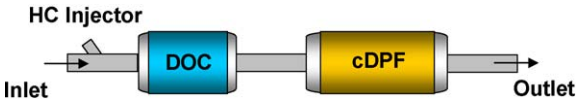

Fig. 1. Assembly of aftertreatment system.

Thermal deactivation is also induced by interactions of active sites with washcoat (mostly aluminium oxide Al_2O_3) and the formation of less active metal alloys [3]. Phase transformation of the porous support γ-Al_2O_3 to the most stable non-porous α-Al_2O_3 results in encapsulation of the active metal sites and in turn to performance deterioration [4]. Adding several additives like BaO, CeO_2 and La_2O_3 to the washcoat leads to a stabilization of the washcoat and less support sintering [5].

Contrary to thermal deactivation of catalysts, the performance loss due to poisoning occurs at lower temperatures. It is caused by deposition of poisoning elements such as phosphorous, sulphur, zinc or magnesium coming from fuel or lubrication oil on the catalyst surface. Chemical poisoning distinguishes between non-selective and selective poisoning. In both cases the accessibility of the catalytically active noble metal sites is reduced [5,6]. The main deactivated zone caused by poisoning elements is the entry zone of the catalyst. Generally, poisoning is a slow and irreversible process. However, sulphur can partly be desorbed again from the catalyst surface by increasing exhaust gas temperature.

For the investigation of the deactivation of catalysts, different methods are used. The cheapest and fastest method is thermal or hydrothermal oven ageing, i.e. exposure to a constant high temperature for a defined time. However, with this solely thermal ageing phenomena can be investigated. More information on the activity loss of catalysts can be gathered by the evaluation of on-road or test bench aged catalysts. These catalysts are affected by a combination of thermal aging and chemical poisoning.

3. Catalyst samples

To get a better understanding for ageing phenomena, DOCs from several combined aftertreatment systems aged in endurance run either on test bench or on-road were investigated and compared to a reference conditioned DOC. Two test bench and five vehicles aged DOCs were analyzed. The DOCs were run in the assembly shown in Fig. 1, consisting of a combination of DOC and cDPF (coated Diesel Particulate Filter).

A HC injector is located in front of the DOC. Liquid HCs are injected into the exhaust gas and heat is generated by their exothermal combustion on the DOC. The resulting high temperature is used for the active regeneration of the downstream cDPF.

Some information on each aftertreatment system influencing the thermal and chemical ageing processes is given in Table 1, e.g. operation time, number of active DPF regenerations, oil consumption and sulphate ash content of the engine oil. For the endurance runs different engines were used, all medium duty class (300–330 hp).

The two test bench aged systems were aged on a test cycle consisting of full load points only. Therefore these systems have seen relatively high exhaust temperatures and high exhaust gas mass flows not only during active DPF regeneration, but also during normal operation mode. System 5 is the system with the highest engine oil consumption. Therefore this DOC was exposed to the highest amount of poisoning elements. System 6 was stressed with the most active DPF regenerations and therefore spent the longest time at very high temperatures. For all systems, each active DPF regeneration lasted 26 min with an end temperature around 600 °C at the DOC outlet face. The regeneration strategy is based on a time controlled temperature ramp. Even higher temperature peaks inside the DOCs and cDPFs can appear through changes in the load profile (e.g. drop to idle) during active DPF regenerations. The geometric dimensions and other parameters of the investigated DOCs are summarized in Table 2.

The two types of DOCs investigated differ in diameter and thus in total PGM loading. Specific PGM loading is 41.25 g/ft^3 for both types. All DOCs are zone coated the front half with 55.8 g/ft^3 PGM and the rear half with 26.8 g/ft^3 PGM, respectively. The DOC of system 6 is the only catalyst with a diameter of 9 in. and therefore of type 1, all other DOCs in this study are of type 2.

After the endurance runs, all DOCs were evaluated on the same test bench engine. NO_2 conversion was measured at two different engine speeds (1100 and 2200 rpm) and different loads. After the first evaluation, "heat up" experiments were run with DOC outlet temperatures around 600 °C. After that, all DOCs were conditioned at 450 °C for 2 h on test bench and then re-measured in the load points at the higher engine speed of 2200 rpm.

4. Test bench results

NO_2/NO_x behind the different DOCs was evaluated and in the following shown as a function of active DPF regeneration time. In Fig. 2 the NO_2 conversion is shown at a DOC inlet temperature of 270 °C and a space velocity of 52,726 1/h.

With an increasing number of active DPF regenerations and therefore total active regeneration time, NO_2 make decreases asymptotically. Maximum ageing duration investigated was 998 h of active regeneration time. A stabilization of catalyst behaviour can be seen after approximately after 600 h of active DPF regeneration time. More regenerations lead only to marginally higher performance loss. DOC 3 (test bench aged) and DOC 7 (on-road aged) with approximately the same number of active DPF regenerations show a similar NO_2 make. As described, for some systems (e.g. DOC 5) repeat measurements were undertaken after heat up tests and a conditioning process. These values show some variation. This might be caused by soot and HC deposits from the endurance run still on the respective DOCs before the first measurement.

Fig. 3 shows the NO_2 conversion at a lower space velocity but same DOC inlet temperature. The relatively low NO_2 make of reference DOC 1 is probably caused by an insufficient conditioning

Table 1
Additional information about exhaust gas aftertreatment systems.

	Cycle	Status	Endurance run time	# Act. reg.	Act. reg. time [h]	Oil consumption [l]	Oil sulphate ash cont. [w%]
System 1	Reference	Conditioned	–	–	–	–	–
System 2	Full load points	Aged	557 h	390	169	17.02	1.096
System 3	Full load points	Aged	1017 h	631	273	36.09	1.096
System 4	On-road	Aged	77,254 mls	890	386	53.92	1.26
System 5	On-road	Aged	152,503 mls	1184	513	71.57	1.26
System 6	On-road	Aged	100,032 mls	2303	998	58.33	1.26
System 7	On-road	Aged	75 tkm/1900 h	649	281	26.65	1.133
System 8	On-road	Aged	90,992 mls	897	389	47.55	1.133

Table 2
Catalyst parameters.

	DOC 1	DOC 2
Size, $D \times L$ [in. × in.]	9 × 6	10.5 × 6
Volume [L]	6.25	8.51
Cell density [cpsi]	300	300
Wall thickness [mil]	5	5
Wash coat	Aluminia based	Aluminia based
PGM loading [kg/m^3]	1.457	1.457
PGM loading [g/ft^3]	41.25	41.25
Pt:Pd	10:1	10:1

procedure before the beginning of the evaluation (10 h at 400 °C in thermal oven). In this load point, no re-measurements were made. Under these conditions, also an asymptotic behaviour of ageing deterioration can be seen.

Generally at an exhaust gas temperature of 270 °C reaction kinetics is fast and also space velocity in the investigated order of magnitude is not limiting.

In Guethenke et al. [7] some more results of this study are shown, including further load points and more DOCs, and also an oven aged component.

5. Chemical and physical laboratory investigations

All aged DOCs and the reference DOC were investigated by post mortem analyses. The aim of the post mortem analysis is to gather more detailed information about the phenomena causing thermal and chemical ageing. As investigations methods BET (Brunauer-Emmett-Teller), XRF (X-ray fluorescence), XRD (X-ray diffraction) and FESEM-EDX (Field emission scanning electron microscopy–energy dispersive X-ray) were used.

Table 3
Overview of the methods for post mortem analysis.

Method	# Samples	Position
BET	6	1A, 1B, 1B2, 1B3, 1C, 1D
XRF	6	1A, 1B, 1B2, 1B3, 1C, 1D
XRD	4	4A2, 4B2, 4C2, 4D2
FESEM/EDX	4	4A1, 4B1, 4C1, 4D1

Before post mortem analyses were started, all DOCs were conditioned in a thermal oven to burn off possible soot accumulation on the catalyst surface. For the different methods several samples from each investigated DOC were prepared. An overview of the methods and the number of samples is given in Table 3.

The position of samples for each investigation method is shown in Fig. 4.

To gain access to the sample positions all DOCs were quartered. Quarters 1 and 4 of each DOC were used for the investigations. The samples A and B were taken from the DOC inlet side, and all C and D samples from the DOC outlet side.

To determine the specific surface area, the BET method certified by DIN ISO 9277 was applied. Nitrogen was used as adsorption gas. Fig. 5 shows the results of the BET measurements.

The results from the BET analysis show that the specific surface area differs in each sample position for a single DOC. The BET measurements were conducted on the washcoated substrates. Specific surface area is mainly provided by the porous washcoat. Variations in the specific surface area for a single DOC can be caused by variations in washcoat thickness and/or wall thickness of the substrate.

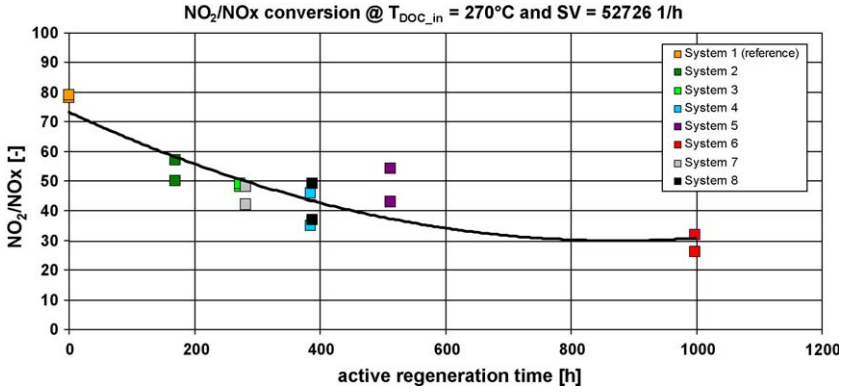

Fig. 2. NO_2/NO_x @ T_{DOC_in} = 270 °C and SV = 52,726 1/h.

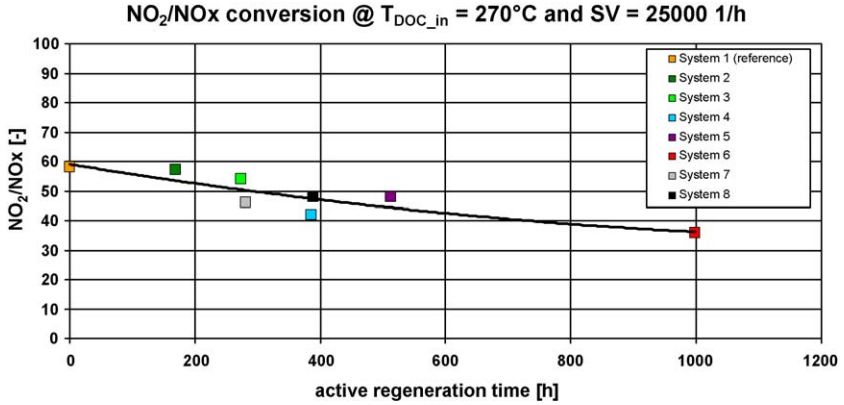

Fig. 3. NO_2/NO_x @ T_{DOC_in} = 270 °C and SV = 25,000 1/h.

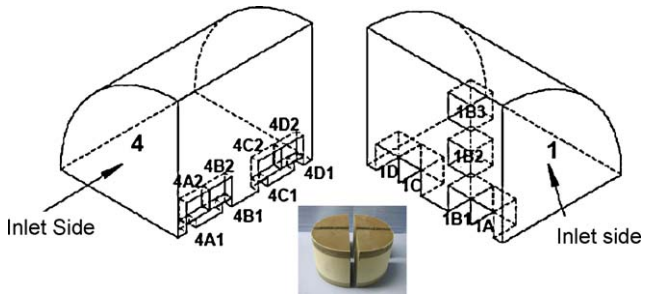

Fig. 4. Position of samples.

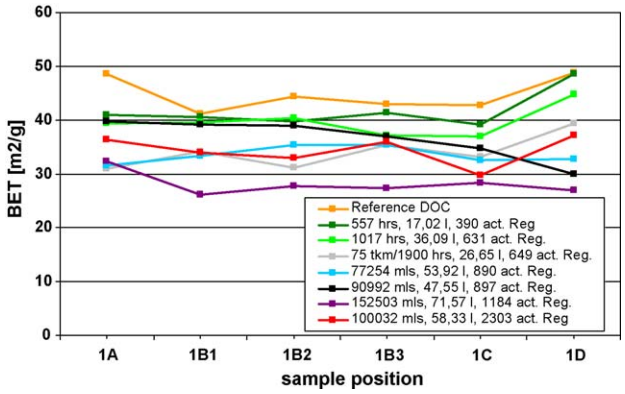

Fig. 5. BET results.

As can be seen, the BET values for the different DOCs vary from each other. The reference DOC (orange) has the highest surface area, having seen no active DPF regenerations. Generally a decrease in specific surface area with increasing number of active regenerations is apparent. However, no direct correlation between the number of active DPF regenerations and the decrease in the specific surface area can be found. A further influence factor on BET surface can be the temperature profile during the durability run driving cycle.

For example the DOC with the highest number of active DPF regenerations (red line) has a higher specific surface area than DOC 5 (violet line) with half the number of regenerations but higher operation time.

After the BET investigations the same samples were used for XRF analysis. With XRF the concentrations of elements are determined by evaluation of the X-ray fluorescence radiation of each element. In this case a quantitative screening of 20 elements on smelted samples was performed, which did not include Pt. To also determine the Pt content, a semi-quantitative analysis on powder samples was performed as well. In the following diagrams the content of oxides of the main poisoning elements (phosphorous, sulphur, zinc and calcium) and of Pt as well as their accumulation behaviour over the DOC length for DOC 1 (reference DOC) and DOC 4 (highest phosphorous accumulation) is shown exemplarily.

The reference DOC shows a very low accumulation of poisoning elements due to the short operation time as seen in Fig. 6. Only sulphur is accumulated on the surface. The axial Pt distribution is in line with the zone coating of the DOC. CaO belongs to the trace constituents of cordierite. Therefore the detection of CaO in the samples is presumably traced back to composition of cordierite and not to the additive coming from lubricant oil.

In Fig. 7 the accumulation of poisoning elements on DOC 4 is shown.

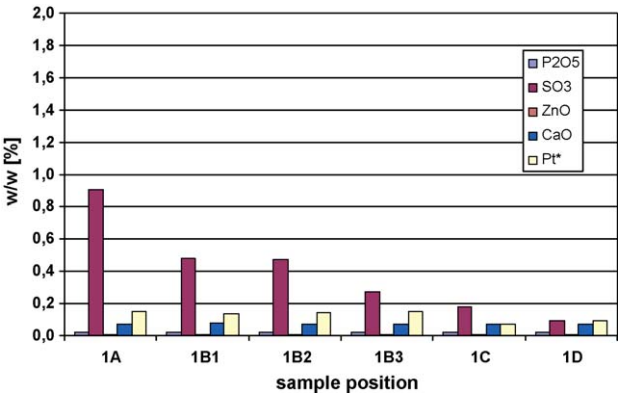

Fig. 6. XRF results for system 1.

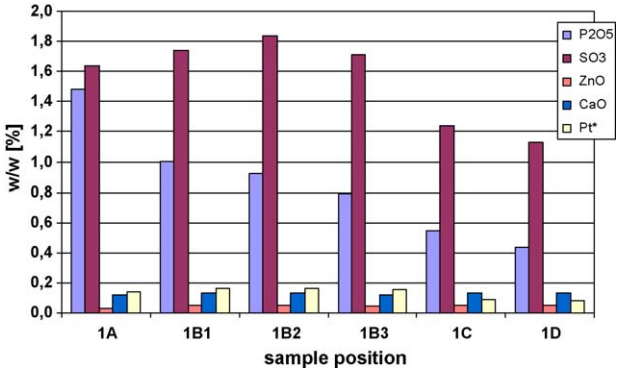

Fig. 7. XRF results for system 4.

An axial and radial distribution profile for phosphorous is visible. The accumulation decreases axially and radially. Sulphur shows a similar behaviour to phosphorous, however the distribution profile is not so clear. Zinc and calcium are poisoning elements with low accumulation concentrations.

The XRF results of the other DOCs are not shown in detail. In general the concentration of the poisoning element sulphur is the highest, whereas often no clear distribution profile is visible. The accumulation of the other poisoning elements on the DOC samples except phosphorous is always very low.

As stated, phosphorous generally shows a clear axially and radially decreasing distribution profile. Fig. 8 shows the values for all investigated DOCs in all sample positions. However the accumulated amount does not correlate with the oil consumption directly. This phenomenon may be attributable to the different driving conditions during the durability runs. The vehicles have

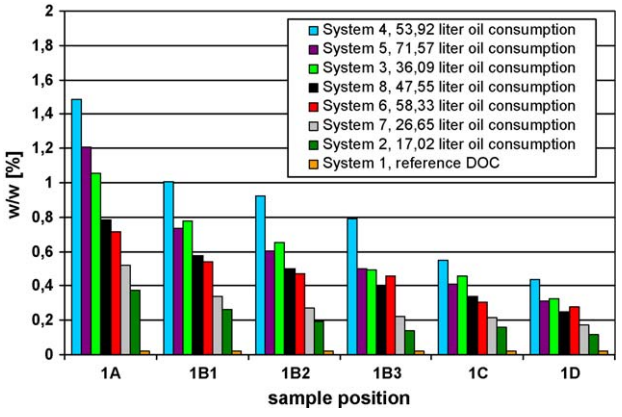

Fig. 8. Distribution profile of phosphorous for all DOCs.

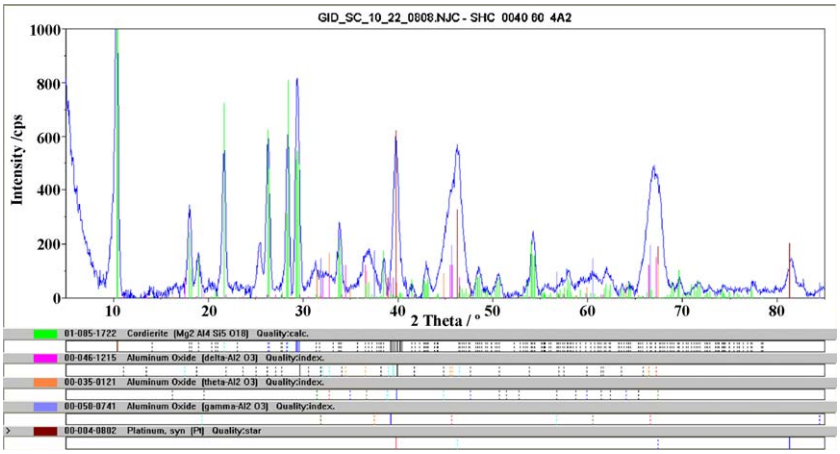

Fig. 9. XRD results for DOC 6 sample 4A2.

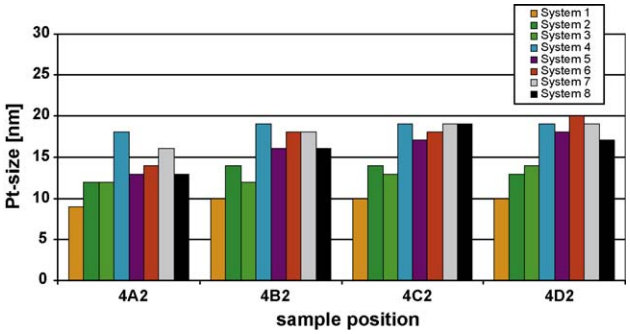

Fig. 10. Pt crystallite size at peak 39.9 2ϑ.

different engine sizes (double and single stage engines) and also the vehicle weight (12–36 tons) is varying.

XRD was used to characterize the crystallographic structure of the DOC samples. To analyse mainly the washcoat composition, a flat angle of incidence (CuKα rays) of 3° was used. In Fig. 9, the XRD diffraction pattern of sample 4A2 from DOC 6 is shown.

The XRD diffraction pattern shows that the washcoat consists of different Al_2O_3 phases. Three different phases are detectable (γ-, δ- and θ-Al_2O_3). The different phases of alumina can occur through the sintering process. All phases are found in the washcoat of the reference DOC as well. Next to the Al_2O_3-phases some Pt-peaks and peaks of cordierite are detectable. Due to the zoning of the DOC, the Pt peaks in its front half are generally higher than the peaks in the rear. All XRD diffraction patterns have a similar shape whereas the intensity of the detected phases changes.

For the evaluation of the ageing status of the DOCs, the Pt crystallite size was evaluated by means of the Scherer equation for the Pt-Peaks at 39.9° and 81.5° 2ϑ. In Fig. 10 the Pt crystallite sizes at 39.9° 2ϑ are shown for all DOCs.

The Pt crystallites on the reference DOC are at all positions the smallest. With increasing number of active DPF regenerations, the crystallite size is growing due to the temperature exposure. However, no direct correlation between the Pt crystallite size and the number of active DPF regenerations is visible. The differing driving conditions during the durability runs may influence Pt crystallite growth.

To determine the qualitative composition and structure of the washcoat layer, FESEM and EDX were used. All samples from 4A1 to 4D1 of each DOC were investigated. On three points of the washcoat, detailed photos with different magnifications (20,000 up to 50,000) were taken. The washcoat was analyzed at the edge, the center and close to substrate wall. The positions for FESEM analysis are shown in Fig. 11.

On all aged DOCs, several Pt crystallite particles bigger than 10 nm were detected. The average particle size over all investigated samples of the reference DOC is being ca. 16 nm. On DOC 4 at position 4D1 (Fig. 11), a Pt crystallite particle with even 122 nm was found. For all DOCs investigated the size of Pt crystallite particles increases along the axial DOC length. Generally the

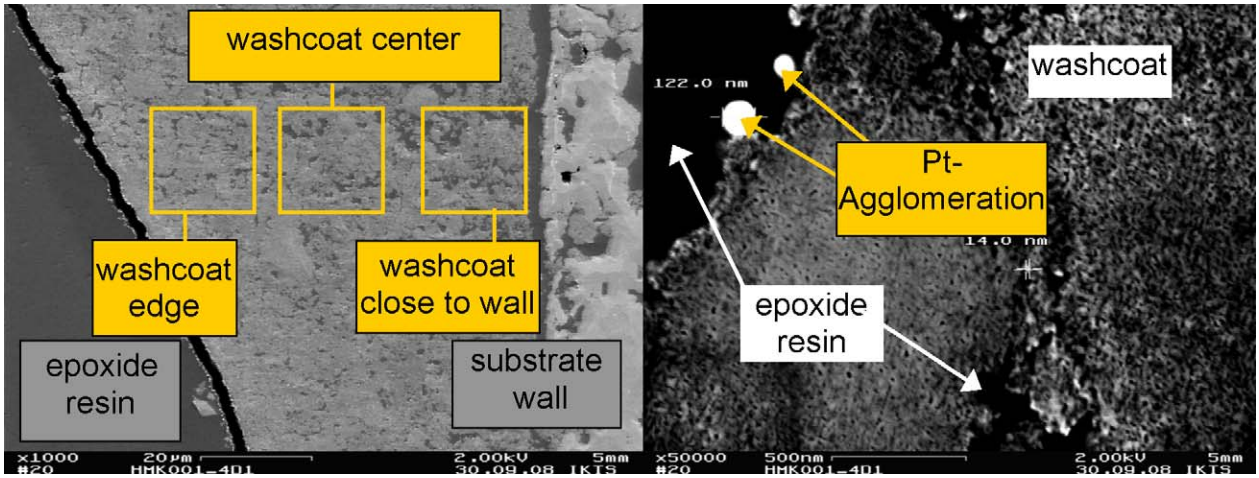

Fig. 11. FESEM investigations at position 4D1 of system 4.

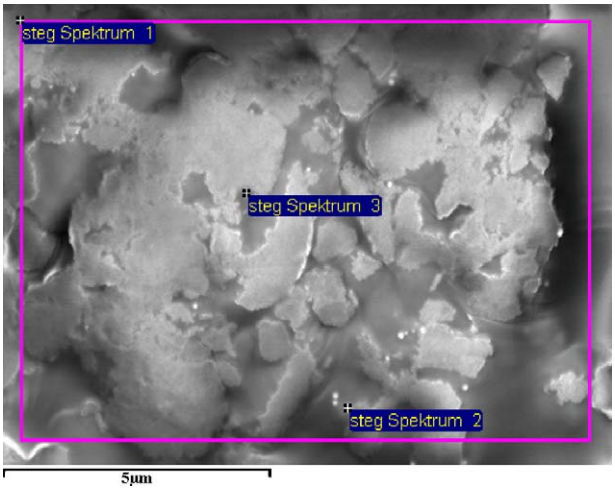

Fig. 12. EDX spectrum at sample position 4D1 of system 4 (washcoat close to wall).

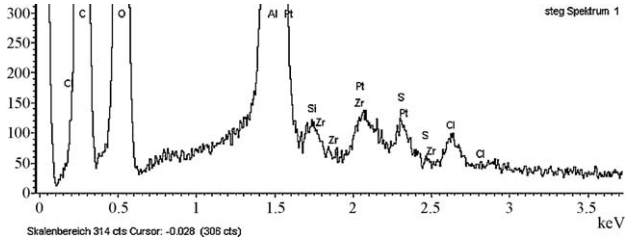

Fig. 13. EDX spectrum 1 (overview) at position 4D1 of system 4.

biggest particles are found at the DOC outlet side (sample position 4D1). This is in agreement with the XRD analysis (Fig. 10). In comparison to all aged DOCs, the located crystallite particles on the reference DOC are much smaller.

At the investigated positions, additionally EDX analyses were carried out. EDX analysis was performed at a voltage of 15 kV. In this range of voltage, nano particles with a size of 20 nm are visible and detectable. Planimetry EDX analyses were done at a magnification of 10,000. Additionally spot measurements on single Pt crystallite particles were performed. By these spot measurements, the neighbouring area (ca. 3 mm) is investigated as well. The resolution limit of the elements is 1–2 w/w%.

In Fig. 12 the EDX spectrum overview (spectrum 1) and the positions for the spot measurements (spectra 2 and 3) are shown.

The EDX spectrum 1 (overview) at position 4D1 of system 4 is shown in Fig. 13. In general it was possible to locally detect trace elements of Pt, Pd, S and P with EDX. Due to peak overlapping of Pt and P at 2.1 keV it is difficult to detect P clearly. The detected elements chlorine and carbon do not originate from the investigated samples, but from the epoxide resin which was used for stabilization of the nano particles.

6. Conclusions

The conversion activity of catalysts is mainly influenced by the accessible catalytically active noble metal surface distributed on the washcoat and is therefore enhanced by small noble metal particle sizes. With increasing operation time and the exposure to high exhaust gas temperatures during active DPF regenerations, the noble metal surface as well the specific surface area of the washcoat decreases. These phenomena lead to catalyst deactivation. The deposition of poisoning elements originating from engine oil also leads to an activity loss of the catalyst. This type of poisoning is a slow process and gains importance with increasing operation time.

In this study, several DOCs were investigated regarding these phenomena. Altogether two test bench aged DOCs and five on-road aged DOCs were compared to a reference DOC. The NO_2 conversion efficiency of each DOC was measured in different operation points on test bench. With increasing number of active DPF regenerations, performance decrease shows an asymptotic behaviour. A stabilization regarding NO_2 make can be seen after approximately 600 h of active DPF regeneration time.

Additional post mortem analyses of the DOCs were performed to further investigate thermal and chemical ageing phenomena. BET, XRF, XRD and FESEM/EDX analyses were made to analyse the structure and composition of each DOC. BET results show that the specific surface area decreases with increasing number of active DPF regenerations, but no direct correlation could be determined.

The accumulation of the poisoning elements on the DOC originating from engine oil was investigated with XRF. Phosphorous shows axial and radial deposition profiles, with decreasing concentrations along the DOC length and radius. However, a clear correlation with the amount of oil consumed could not be determined. Sulphur shows more changing profiles, as its deposition is reversible and more susceptible to temperature and therefore active DPF regeneration history. Other poisoning elements can only be seen in minor concentrations.

XRD as well as FESEM investigations show that Pt crystallite size increases with the number of active DPF regenerations and the crystallite size is bigger towards the DOC outlet face than at the inlet, as temperatures at the inlet are lower during active DPF regenerations.

Overall, the data analysis was complicated by the large number of influence factors during on-engine ageing (vehicle weight, total lube oil consumption, number of active DPF regenerations, etc.), leading to different influences on thermal and chemical ageing phenomena and therefore hindering the development of clear correlations.

Further investigations on a larger number of aged DOCs will follow to clarify and further differentiate between the ageing phenomena observed. Also, thermal and chemical effects on catalytic conversion deterioration will be analyzed separately. Therefore, oven aged components as well as components exposed to a higher level of poisoning elements will be investigated.

Acknowledgments

The authors thank Dr. Petasch, Fraunhofer IKTS, for the measurements supporting this work.

References

[1] C.H. Bartholomew, Applied Catalysis A 212 (2001) 17.
[2] J.B. Butt, et al., Activation, Deactivation and Poisoning of Catalysts, Academic Press Inc., 1988.
[3] R.J. Brisley, SAE Tech. Pap. Ser. 910175 (1991).
[4] A.K. Neyestanaki, et al. Fuel 83 (2004) 395–408.
[5] R.M. Heck, et al., Catalytic Air Pollution Control, Van Nostrand Reinhold, NY, 1995.
[6] G.C. Bond, Heterogeneous Catalysis, Clarendon Press, Oxford, 1987.
[7] A. Guethenke, et al., SAE Tech. Pap. Ser. 2009-01-0623 (2009).